

---

EFDA–JET–CP(03)01-21

A. Géraud, L. Garzotti, P. T. Lang, A. Lorenz, B. Pégourié, G.L. Schmidt,  
B. Alper, T.T.C. Jones, P. Monier-Garbet, J. Strachan, M. Stamp, P. Bennett,  
J. L. Maréchal, R. Mooney, J. Ongena, M. J. Watson, D. J. Wilson  
and JET EFDA Contributors

# Experimental Comparison of Different Configurations of Injection for Pellet Fuelling on JET



# Experimental Comparison of Different Configurations of Injection for Pellet Fuelling on JET

A. Géraud<sup>1</sup>, L. Garzotti<sup>2</sup>, P. T. Lang<sup>3</sup>, A. Lorenz<sup>3</sup>, B. Pégourié<sup>1</sup>, G. L. Schmidt<sup>4</sup>,  
B. Alper<sup>5</sup>, T. T. C. Jones<sup>5</sup>, P. Monier-Garbet<sup>1</sup>, J. Strachan<sup>4</sup>, M. Stamp<sup>5</sup>,  
P. Bennett<sup>5</sup>, J. L. Maréchal<sup>1</sup>, R. Mooney<sup>5</sup>, J. Ongena<sup>6</sup>, M. J. Watson<sup>5</sup>,  
D. J. Wilson<sup>5</sup> and JET EFDA Contributors\*

<sup>1</sup>Association EURATOM-CEA, CE Cadarache, 13108 St Paul-Lez-Durance, France

<sup>2</sup>Consorzio RFX, EURATOM-ENEA-CNR Association, 35137 Padova, Italy

<sup>3</sup>Max-Planck-Institut für Plasmaphysik, EURATOM Association, 85748 Garching, Germany

<sup>4</sup>PPPL, Princeton, New Jersey, USA

<sup>5</sup>EURATOM-UKEA Association, Culham, Abingdon, Oxon. OX14 3DB, UK

<sup>6</sup>LPP/ERM-KMS, Association EURATOM-Belgian State, B-1000 Brussels, Belgium

\*See Annex of J. Pamela et al., "Overview of Recent JET Results and Future Perspectives",  
*Fusion Energy 2000 (Proc. 18th Int. Conf. Sorrento, 2000)*, IAEA, Vienna (2001).

Preprint of Paper to be submitted for publication in Proceedings of the  
EPS Conference on Controlled Fusion and Plasma Physics,  
(St. Petersburg, Russia, 7-11 July 2003)

“This document is intended for publication in the open literature. It is made available on the understanding that it may not be further circulated and extracts or references may not be published prior to publication of the original when applicable, or without the consent of the Publications Officer, EFDA, Culham Science Centre, Abingdon, Oxon, OX14 3DB, UK.”

“Enquiries about Copyright and reproduction should be addressed to the Publications Officer, EFDA, Culham Science Centre, Abingdon, Oxon, OX14 3DB, UK.”

## INTRODUCTION

The capability of frozen hydrogenic pellet injection to reach high density together with high confinement regimes is of crucial interest for ITER. Furthermore, the associated good fuelling efficiency is important to the tritium cycle, allowing its inventory in the machine to be minimised. However, since the first demonstration in ASDEX-Upgrade [1] that the ablated matter from the pellets experiences a fast drift in the direction of increasing major radius, the optimisation of the injection configuration is still an important issue. The “standard” Low Field Side (LFS) injection is clearly the worst situation since the drift expels the matter out of the discharge. In JET, a first guide tube system has been installed in 1999 to convey the pellets to the High Field Side (HFS) to take advantage of the favourable drift [2]. The injection system has been completed recently with another guide tube, hereafter referred to as Vertical High Field Side (VHFS). Due to larger radii of curvature and more vertical injection directed towards the plasma centre, pellets were expected to be launched at higher speed and to avoid a trajectory tangential to the magnetic surfaces at large minor radii, as was the case with the first track. In this paper, results of first experiments aiming to compare the three available configurations are presented.

### 1. EXPERIMENTAL CONDITIONS AND TRACK CHARACTERIZATION

Using the JET centrifuge injector (delivery efficiency of ~80% at the injector exit), successive trains of 4mm cubic pellets (or about 2/3 size in some cases) were injected at a frequency of 5 Hz into steady, moderately heated (4MW ICRH, 1.4MW NBI) L-mode plasmas. The three different tracks (stainless steel,  $\Phi$  10mm) have been used during the same pulse by means of a fast selector. The corresponding trajectories in the plasma are shown in Fig.1. Pellet velocities between 150 and 400m/s have been explored. The results are presented in Fig.2 which gives, versus injection velocity, the fraction of intact pellets seen in the plasma by the FIR interferometer density diagnostic relatively to the number of pellets detected at the centrifuge exit. The sample analysed consists of 230 pellets fired in 12 different JET pulses (10 to 32 pellets per point). Figure 2 also shows that this first study of the VHFS pellet track almost follows the test results observed at ORNL [3]. Data from the HFS track suggest an improvement of the critical speed to more than 250m/s, a large improvement with respect to  $v = 160$ m/s used in previous experimental campaigns. The difference may be due to the criterion used to sort pellets. Photos were used in laboratory, but in this study pellets have been considered as broken when the plasma density jump was abnormally reduced when normalized to the measured mass at the centrifuge exit. So, pellets broken in only two or three grouped pieces can be considered as unbroken, which is confirmed by the structure of some ablation Ha signals. Reduced size pellets were also injected into the plasma, however, they seem to break at lower speeds of about 250m/s in the VHFS track, possibly due their shape leading to increased bouncing and spiralling in the guide tube. Further experiments are planned to verify these preliminary results.

Pellet mass losses through all three guide tubes were estimated as the ratio of the pellet mass measured by the microwave interferometer to the mass arriving in the plasma deduced from the instantaneous (available time resolution  $\Delta\tau = 1$ ms) particle plasma content jump. Figure 3 shows the

losses as function of pellet speed and track configuration. The data do not include centrifuge losses and are referenced to pellets injected from the LFS track at 155m/s. Whereas the mass loss are expectedly small through the short LFS tube, they increase strongly with speeds in particular in the HFS tube, although it is 1.5 times shorter than the well pumped VFS tube. This is in line with observations at ASDEX Upgrade [3], where efficient evacuation of evaporated pellet material in the guiding tube was found to mitigate significantly runaway mass losses in tubes at high pellet speeds.

## 2. FUELLING CAPABILITY

The analysis of the fuelling is done in terms of increase and relaxation time of the plasma electron content. Typical traces are presented in Fig.4 (JET Pulse No: 58337), in which the three configurations have been used. The pellet velocity was 250m/s with particle content constant at the centrifuge exit (within 10%), but not measured at the tracks exit. A specific calculation of the plasma particle content jump (fig.4(b) has been done from the raw data of the interferometer in order to take advantage of the fast data acquisition. With a resolution time  $\Delta\tau$  in the range 1-7.5ms, the diffusive loss of particle between two measurements is negligible. Nevertheless, in the LFS case, the fast relaxation (corresponding to a decrease of 2-3  $10^{20}$  electrons in the plasma particle content) requires  $\Delta\tau < 2-3$ ms to be seen reliably. This is illustrated in Fig.5(a), where the relaxation of the plasma content, normalized to its maximum just after each injection, is plotted for the three configurations. In all the discharges analysed, the  $\Delta\tau = 1$  ms acquisition window was limited to 2s ((18.5s-20.5s) for JET Pulse No: 58337), making difficult the comparison of the different cases. As a consequence, in Fig.4(b), the increment of the plasma content for the LFS case must be corrected by the fast loss component (up to 2-3  $10^{20}$ ), yielding an average value of about 1.5  $10^{21}$  electrons. The density increment for pellets injected from the VHFS exhibits a reduction of 35% with respect to the LFS case, due to the erosion of the pellets in the guide tube, and the degradation is yet larger for the HFS pellets, due to a larger erosion (Fig.3). The relaxation of the total number of electrons in the plasma is compared for the 3 configurations in Fig.5(a) : it is the same for the HFS and the VHFS configurations, the difference between the LFS and (V)HFS cases reflecting the effective source location. Fig.5b shows this relaxation as a function of the pellet speed for the VHFS track and for similar target plasmas, confirming the favourable dependence of the effective depth of the source on the injection speed.

## 3. COMPARISON OF THE MATTER DEPOSITION PROFILES

The ablated material deposition profile is measured by the LIDAR diagnostic. Typical pre- and post-injection profiles in the three configurations are shown in Fig.6. As far as the profile of density increment is concerned, the HFS and VHFS configurations appear similar. The pellets ablation and deposition profiles are simulated by means of two codes integrating ablation (NGPS scaling [4]) and  $\nabla B$ -drift effect. The first one is similar to that described in [5], but allows for non-circular geometry and off-axis injection. For HFS launched pellets, it takes into account the pre-cooling of the plasma by the material deposited previously and drifting in front of the pellet. The distance of drift itself is assumed

to be constant in the whole plasma cross-section and equal to 25-30cm. The second [6] calculates self-consistently the homogenization of the ablated material simultaneously with the  $\nabla B$ -induced displacement, but does not take into account a possible pre-cooling. The major feature of this more detailed calculation is that the distance of drift is smaller for HFS launched pellets (drift towards increasing plasma pressure) than for LFS launched pellets (drift towards decreasing pressure). This is the reason of the difference between the two calculations in the LFS case (fuelling efficiencies  $\eta$  of ~80 and ~50 %, respectively), when the two simulated sources are in reasonable agreement for the HFS and VHFS cases ( $\eta > 90\%$ ). In what concerns the comparison with measurements, the agreement is reasonable in the HFS and VHFS cases (deposition radius and magnitude of the density increment). The comparison is more difficult in the LFS case, due to the long time delay (40ms) between injection and LIDAR measurement. Finally, it is clear that the experimental deposition profiles are wider than the calculated ones by a factor hardly explained by standard radial transport during this long time interval. This suggests a possible link between the homogenization of the ablated material and a phase of increased radial transport in the plasma.

#### **4. FIRST RESULTS OF A NEW HIGH TIME RESOLUTION SPECTROMETER**

A high time resolution spectrometer has been installed to monitor ablation cloud density for use in modelling the pellet mass redistribution mechanism [7]. First measurements, which were also done in H-Mode plasmas are shown in Fig.7 (integration time 500ms) : cloud densities are observed to increase with penetration depth [8]. For HFS injection, density is generally lower for L-Mode at moderate power (JET Pulse No: 58337) than for H-Mode at high power (JET Pulse No: 55340). Measurements of density for the LFS trajectory are limited by viewing constraints; but in L-mode, density appears to be comparable to the HFS H-Mode case and greater than the HFS result for similar L-Mode plasmas.

#### **CONCLUSIONS.**

The first experiments of pellet injection performed with the new VHFS track allowed to determine the range of acceptable conditions for a reliable fuelling. In the present configuration, a maximum pellet speed of at least 350 m/s is found, as expected from laboratory tests [3]. In addition we have demonstrated that the HFS track can be used at speeds up to about 250m/s with a good fuelling capability, which is larger than used in previous pellet experiments.

For the L-mode experiments carried out during this first campaign, the VHFS and HFS tracks exhibit the same fuelling properties. The same deposition profile is deduced from the LIDAR measurements for HFS and VHFS pellets injected into similar plasmas. This is compatible with the predictions of the simulations, particularly the moderate  $\nabla B$ -drift, consistent with the low  $b$  plasmoids produced in these L-mode experiments.

## REFERENCES

- [1]. Lang, P.T., et al., Phys Rev Lett **79** 8 (1997) 1487
- [2]. Jones, T.T.C., et al., ECA Vol. 24B (2000) pp 13-16
- [3]. Lorenz, A., et al., Fusion Engineering and Design, 20th SOFT, Helsinki 2002 in print
- [4]. Garzotti L., et al., Nucl. Fusion **37** (1997) 1167.
- [5]. Pegourie B. and Garzotti L., ECA 1997, vol. 1., 152.
- [6]. Waller V., et al., paper P-1.145, this conference
- [7]. Parks, P.B., Sessions, W.D., and Baylor, L.R., Physics of Plasmas, Vol.7 (2000), 1968
- [8]. Schmidt, G.L., et al., 44th APS Annual Meeting of the Division of Plasma Physics, Orlando, USA, 11-15 Nov., 2002



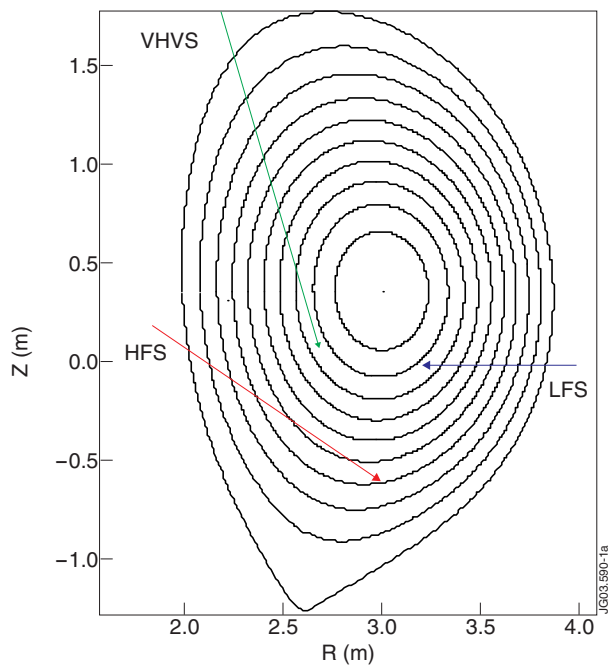


Figure 1 : Trajectories of pellets fired through each of the 3 guide tubes for a typical JET configuration used in the study (JET Pulse No: 58337,  $t=20s$ )

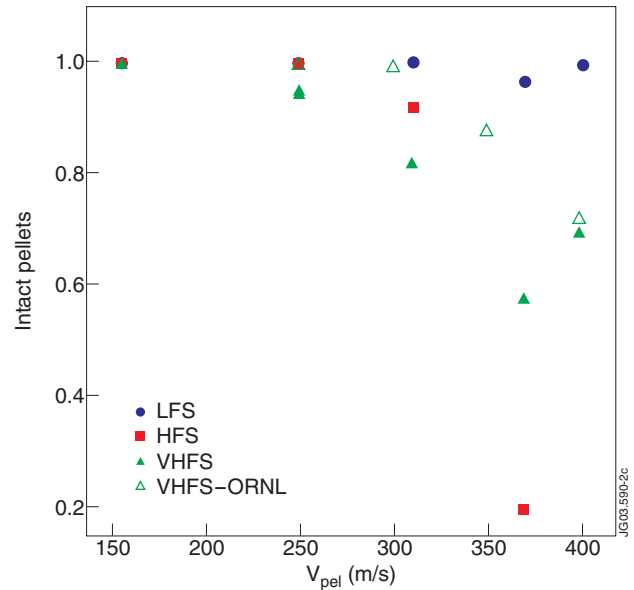


Figure 2 : Fraction of intact pellets detected in the plasma as a function of the pellet speed.

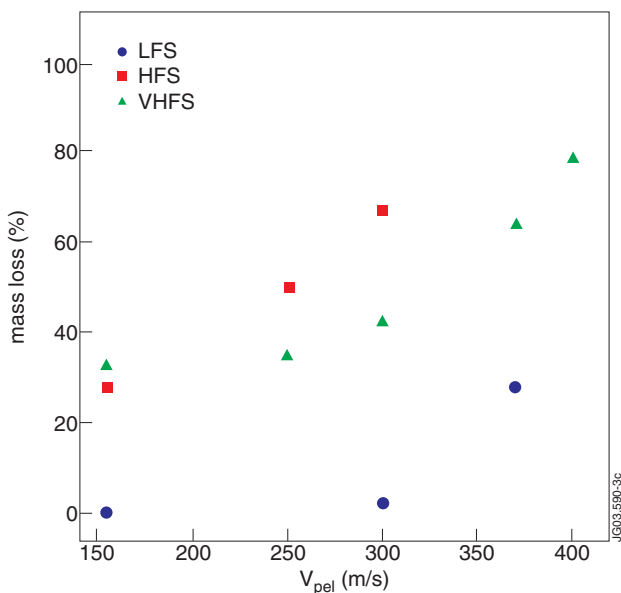


Figure 3 : Mass loss of pellets after passage through different guiding tubes as a function of pellet speed.

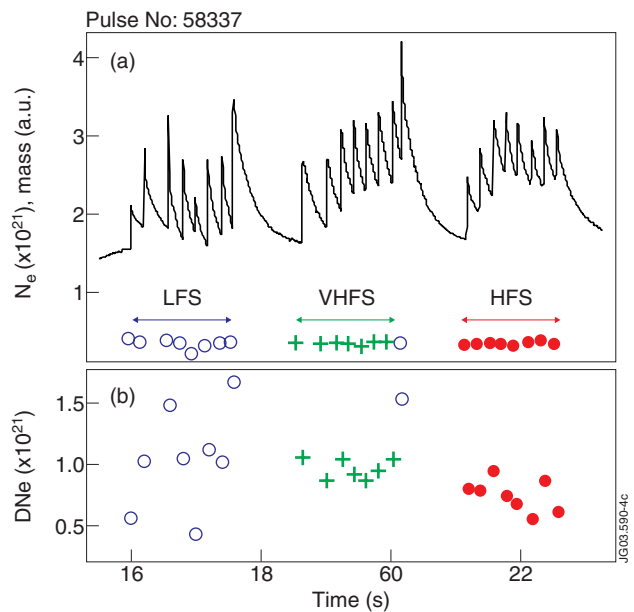


Figure 4 : Time evolution (a) and increment per pellet (b) of the total number of electrons in the plasma for pulse 58337.

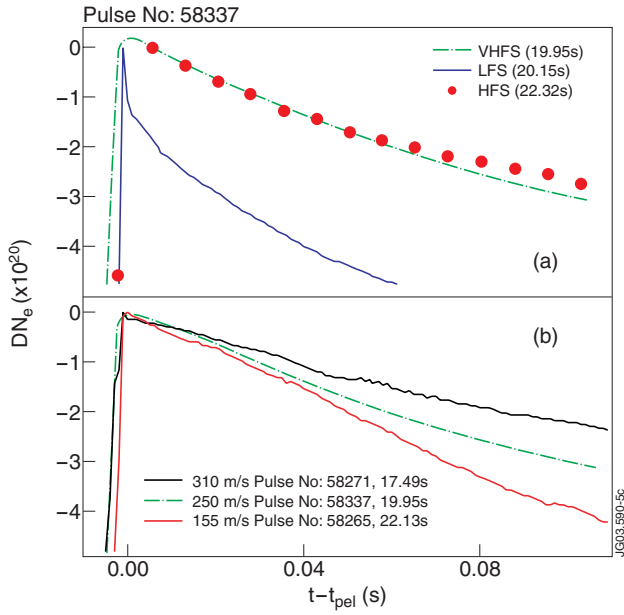


Figure 5: Relaxation of the total number of electrons in the plasma following the ablation of pellets a) from the different tracks ( $v_{pel}=250$  m/s, JET Pulse No: 58337), b) for the new VHFS track at different speeds.

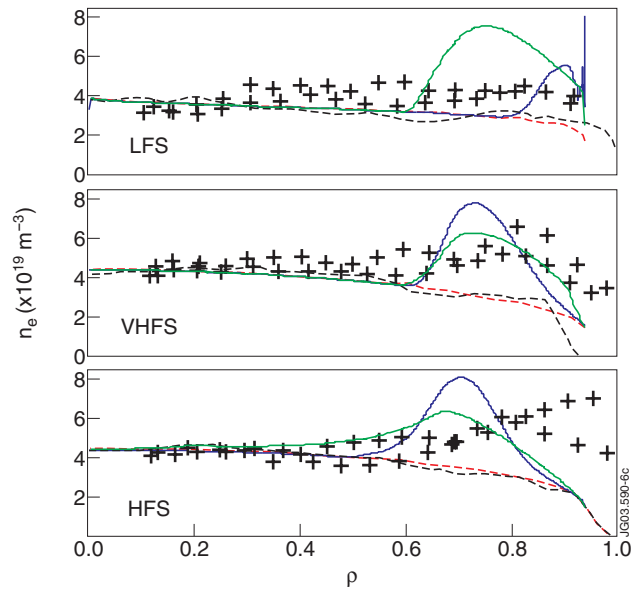


Figure 6: Comparison of the experimental effective matter deposition profiles deduced from the LIDAR (markers, JET Pulse No: 58337, 40ms after ablation for LFS, 10ms for VHFS and 5ms for HFS) with the result of source calculations performed with the empirical ([6], green long-dashed line) and self-consistent ([7], blue solid line) models. Dotted and dashed lines are the LIDAR profiles before injection and the profiles considered in the simulations.

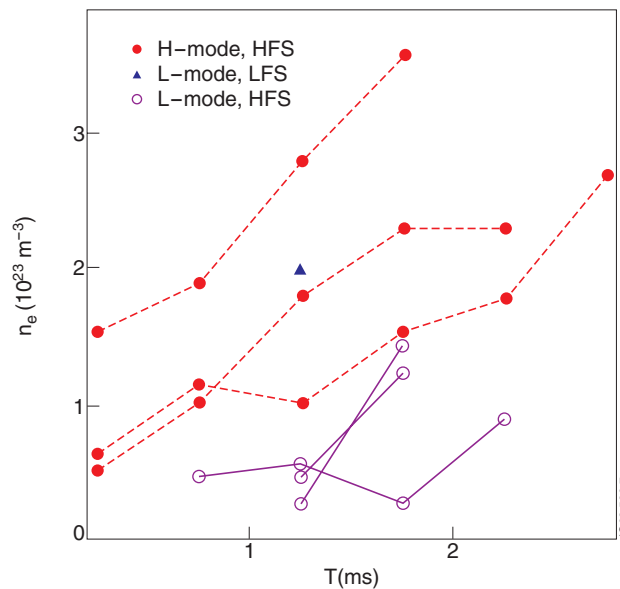


Figure 7: H-Mode, L-Mode time evolution of pellet cloud electron density.